Catalysis Today 148 (2009) 350–354

Contents lists available at ScienceDirect

Catalysis Today

journal homepage: www.elsevier.com/locate/cattod

Synthesis of cyclic carbonate from allyl glycidyl ether and carbon dioxide using ionic liquid-functionalized amorphous silica

Hye-Lim Shim, Seshachalam Udayakumar, Jeong-In Yu, Il Kim, Dae-Won Park *

Division of Chemical Engineering, Pusan National University, Jangeon-dong, Kumjeong-gu, Busan 609-735, South Korea

ARTICLE INFO

Article history:
Available online 21 July 2009

Keywords:
Allyl glycidyl ether
Carbon dioxide
Cyclic carbonate
Amorphous silica

ABSTRACT

Ionic liquid functionalized mesoporous silica (IFMS) was prepared from the coupling of 1-(triethoxysilylpropyl)-3-*n*-alkylimidazolium halides with tetraethyl orthosilicate (TEOS) through template-free condensation under strong acidic conditions. The immobilized ionic liquid (IM-IL) catalysts showed 0.61–0.93 mmol of ionic liquid on SiO_2 and surface area in the range of 189–647 m^2/g with pore sizes from 3.2 to 4.2 nm. Elemental analysis and SEM image showed that the immobilized ionic liquid groups were well incorporated on the support. The silica-supported ionic liquids were proved to be an effective heterogeneous catalyst for the solventless synthesis of cyclic carbonate from allyl glycidyl ether (AGE) and carbon dioxide. Im-IL of longer alkyl chain length and more nucleophilic nature showed higher conversion of AGE. High temperature, high carbon dioxide pressure, and the presence of $ZnBr_2$ co-catalyst were favorable for the conversion of AGE. Im-IL can be reused for the reaction up to three consecutive runs without any considerable loss of its catalytic activity.

1. Introduction

Carbon dioxide is recognized to be a naturally abundant, cheap, recyclable, and non-toxic source of carbon that can sometimes replace toxic chemicals such as phosgene, isocyanates, and carbon monoxide [1–4]. Under these circumstances, chemical fixation of CO_2 becomes more important from both an ecological and an economic point of view. Among them, the application of carbon dioxide as a monomer for the synthesis of various polymers has received much attention in recent years. The reactions of carbon dioxide with oxiranes leading to five-membered cyclic carbonates are well-known examples. These cyclic carbonates can be widely used for various purposes, such as aprotic polar solvents, electrolytes for batteries and sources for reactive polymer synthesis [5].

The five-membered ring cyclic carbonates (1,3-dioxolan-2-ones) are generally incapable of ring opening polymerization due to their thermodynamic stability, but do undergo polymerization with partial loss of CO_2 to yield macromolecules with both ether and carbonate linkages. Due to such uses, a number of syntheses of cyclic carbonates and polycarbonates have been described over the last 30 years [1,6–12].

Many catalytic systems [13–15] were developed for the insertion of carbon dioxide into oxiranes, such as alkali metal salts [16], alkali metal salts combined with crown ethers or quaternary ammonium salts [17], organoantimony halides [18], MgO [19] or Mg–Al mixed oxides [20], ionic liquids [21], porphyrin [22], transition-metal complexes [23], phthalocyanine [24], polyoxometalate [25], supercritical carbon dioxide [26], amorphous silica immobilized ionic liquid/$ZnCl_2$ [27], amine-functionalized mesoporous Ti(Al)-SBA-15 [28], and as-made MCM-41 [29]. However, the processing of homogeneous system limits their application to the catalyst, these catalysts are mainly suffering for separation, reusability and less cost effective process, hence moving to heterogeneous conditions can overcome those problems, but negative sides of these catalysts are low catalytic activity and/or selectivity, low stability, and requiring high pressure. Therefore, the development of a highly efficient solid catalyst system for the chemical fixation of carbon dioxide under mild conditions remains a challenge.

The use of ionic liquids as environmentally benign media for catalytic processes or chemical extraction has become widely recognized and accepted [30]. Ionic liquids have negligible vapor pressure, excellent thermal stability and special characteristics in comparison with conventional organic and inorganic solvents. Many reactions catalyzed with ionic liquids and showing high performance have been reported [31,32]. In particular, ionic liquids based on imidazolium cations and chloroaluminate anions, such as 1-butyl-3-methylimidazolium aluminium chloride ([BMIm]Cl/$AlCl_3$), have attracted growing interest [33,34].

In our previous work [35], the immobilization of ionic liquids onto MCM-41 showed excellent activities for carbon dioxide insertion reactions, however, the use of expensive pore-directing agents and large amounts of organic solvents to remove the

---

* Corresponding author. Tel.: +82 51 510 2399; fax: +82 51 512 8563.
E-mail address: dwpark@pusan.ac.kr (D.-W. Park).

0920-5861/$ – see front matter © 2009 Elsevier B.V. All rights reserved.
doi:10.1016/j.cattod.2009.06.011

templates makes these catalysts impracticable for commercial scale-up. Moreover, the ordering of the mesopores often decreases as a result. These problems could be avoided through the usage of low-cost and highly efficient method for synthesizing organic functionalized amorphous silica. In addition, amorphous silica with rigid cross-linking skeletons, synthesized at higher acidic conditions, could also improve hydrothermal stability [36–39].

In the present work, we report the synthesis of five-membered cyclic carbonate from allyl glycidyl ether and carbon dioxide using immobilized imidazolium salt ionic liquid on amorphous silica prepared by a simple co-condensation through direct hydrolysis of 1-(triethoxysilylpropyl)-3-*n*-alkyl-imidazolium halide and TEOS under strong acidic conditions without the addition of any structure-directing agent. The effects of alkyl chain length, counter anion, $ZnBr_2$ co-catalyst, carbon dioxide pressure, and reaction temperature are discussed for better understanding of the reaction mechanism.

2. Experimental

2.1. Material

Tetraethyl orthosilicate (TEOS, Aldrich), 3-chloropropyltriethoxysilane (ClPTES, Aldrich) and allyl glycidyl ether (AGE, Aldrich) were commercially available, and they were used without further purification. Carbon dioxide with a purity of 99.99% (Hanyu Chemicals) was also commercially available.

2.2. Preparation of immobilized ionic liquid

Imidazole (5.1 g, 79.5 mmol) was dissolved in 75 mL of dry toluene, to which ClPTES (18 mL, 75 mmol) was added and the mixture was refluxed for 12 h under an argon atmosphere. An oil containing 3-(*N*-imidazolyl)propyl triethoxysilane was obtained, and to it added 1-bromobutane, followed by refluxing for another 12 h under argon to yield the 1-(triethoxysilylpropyl)-3-*n*-butylimidazolium bromide. This is denoted as ionic liquid functionalized organosilane (IFOS). The resultant mixture was purified by washing 3–4 times with hexane petroleum to remove any unreacted impurities. The solution was then mixed with 10 mL of ethanol and distilled under vacuum at 10^{-3} Torr to remove excess hexane.

The molar ratio of the constituents in the synthetic mixture was optimized according to our previous report [40]; 0.818 TEOS:0.182 IFOS:5.61 HCl:153.9 H_2O, where TEOS/IFOS ratio was 4.5. In a typical synthesis, a 500 mL polypropylene (PP) bottle, fitted with a wheel-type magnetic bar and brought to 40 °C, was charged with 100 mL of water, followed by 25 mL of 35% HCl. After stirring for 15 min, a clear solution was obtained. Prior to addition of the 8.01 mL of TEOS, it was placed into the open PP bottle and stirred for 3 h at 40 °C for pre-hydrolysis and expulsion of ethanol from the reaction mixture. The 4.64 mL of the ionic liquid functionalized organosilane (IFOS) and ethanol mixture was then added (initial organosilane mixed with 15 mL EtOH in order to avoid errors from the measurement of the more viscous IFOS) into the aforementioned solution and stirred for 24 h at 40 °C, and subsequently heated another 24 h at 60 °C in a hot air oven in the polypropylene bottle. The solid product was recovered and mixed with 50 mL of ethanol, filtered, and dried at 60 °C for 12 h.

2.3. Sample characterization

Surface area, pore volume, and pore size distribution were measured by nitrogen adsorption at 77 K using an ASAP2010 system purchased from Micromeritics. The solvent-extracted samples were degassed at 110 °C and 10^{-5} Torr overnight before the adsorption experiments. The mesoporous volume was estimated from the amount of nitrogen adsorbed at a relative pressure of 0.5 by assuming that all mesopores had been filled with condensed nitrogen in the normal liquid state. The pore size distribution was estimated using the Barrett, Joyner, and Halenda (BJH) algorithm (ASAP2010) built-in software from Micromeritics. Elemental analysis was performed using a Vario EL III whereby 2.0 mg of the samples were subjected to 1100 °C with sulfanilic acid used as the standard. The morphology of the RImX_SiO_2 (R = alkyl, X = halide) mesoporous catalysts was examined by scanning electron microscopy (HITACHI, S-4200, Japan). The samples were coated with gold using an Instrumental Scientific Instrument PS-2 coating unit.

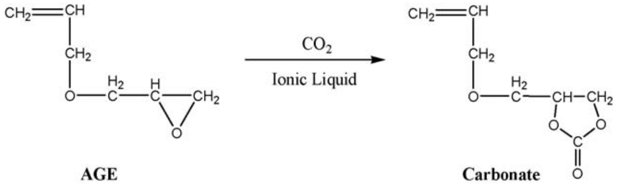

Scheme 1. Synthesis of cyclic carbonate from AGE and CO_2.

2.4. Reactivity test

The RImX_SiO_2 catalyst was weighed in the air (0.5 g) and introduced into a 55 mL high pressure reactor containing 40 mmol of AGE (allyl glycidyl ether) or 2-[(prop-2-en-1-yloxy)methyl]oxirane, under solvent-free conditions, and refluxed in an oil bath at 110 °C with stirring for 6 h under CO_2 atmosphere at a pressure of 0.86–3.55 MPa . A small portion of the reaction mixture was taken to analyze the AGE-concentration by gas chromatography (HP 6890 A) with an HP-1 capillary column. The five-membered cyclic carbonate was confirmed using the authentic sample. Synthesis of the allyl glycidyl carbonate (AGC or 4-[(prop-2-en-1-yloxy)-methyl]-1,3-dioxolan-2-one) from AGE is shown in Scheme 1.

3. Results and discussion

3.1. Characterization of ionic liquid-functionalized mesoporous silica (IFMS)

The N_2 adsorption–desorption isotherm and pore size distribution of the IFMS are illustrated in Figs. 1 and 2. From Fig. 1, the synthesis of various IFMS shows different kinds of hysteresis loops with respect to the nature of the IFOS. Moreover, the nature of IFOS has been classified based on the percentage of hydrophilicity (ionic nature of the aromatic imidazolium group with respect to the counter ion) and hydrophobicity of the alkyl tail (increases with increasing alkyl chain length). The *n*-BImI_SiO_2 has more ionic I^- counter ion and *n*-PImBr_SiO_2 has shorter hydrophobic alkyl chain length than *n*-BImBr_SiO_2, respectively. Hence the IFOS (*n*-BImI-$Si(OEt)_3$) shows better interaction with silica gel it facilitates the incorporation in the framework, however, the IFOS will not contribute to break the gel into emulsion. Therefore, the material can show irregular pore size distribution (Fig. 2, curve a) compared to the optimized *n*-BImBr_SiO_2. These results illustrate that mesoporous structures with narrow pore size distributions can be formed by co-condensation of TEOS with an appropriate amount of IFOS in a strong acidic environment without the addition of pore-directing agents.

The physico-chemical properties of the IFMSs are presented in Table 1. The BET surface area of the *n*-BImBr_SiO_2 was 477.4 m^2/g and that of *n*-BImI_SiO_2 and *n*-PImBr_SiO_2 was 188.9 and 647.4 m^2/g, respectively. The pore diameters are in the range of 3.1–4.2 nm and pore volumes are 0.1–0.4 cm^3/g. Nitrogen content

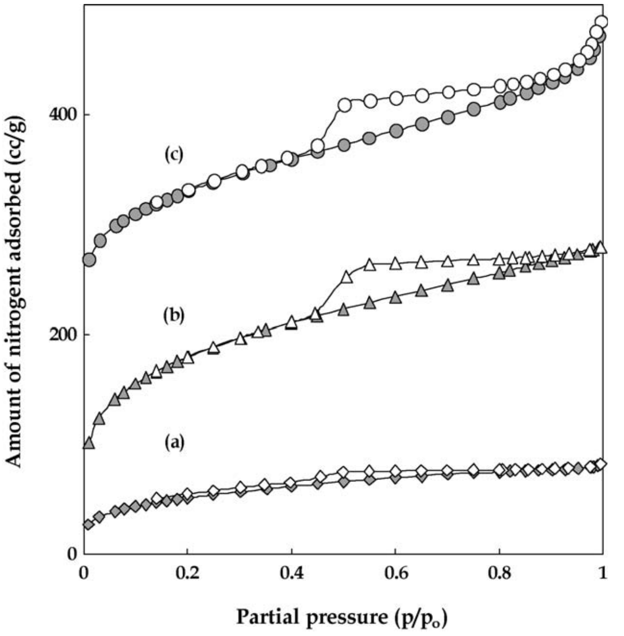

Fig. 1. N_2 adsorption isotherms of RImX_SiO$_2$ (filled symbol for desorption and open symbol for adsorption): (a) *n*-BImI_SiO$_2$, (b) *n*-PImBr_SiO$_2$ and (c) *n*-BImBr_SiO$_2$.

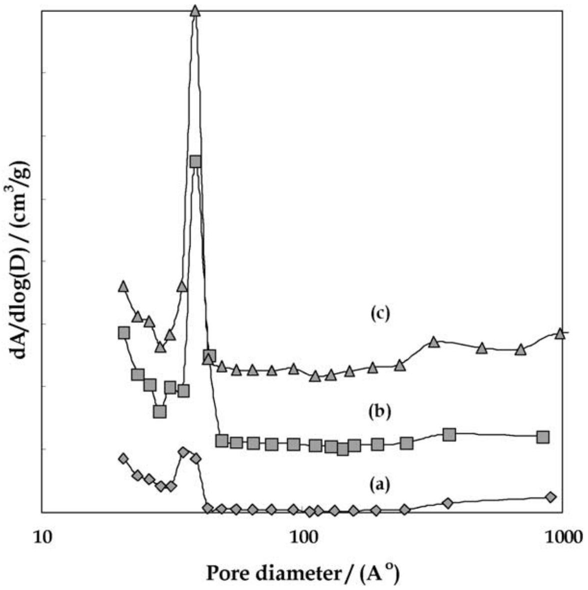

Fig. 2. Pore size distribution for RImX_SiO$_2$ from desorption method: (a) *n*-BImI_SiO$_2$, (b) *n*-PImBr_SiO$_2$ and (c) *n*-BImBr_SiO$_2$.

in the IFMSs was analyzed by elemental analysis, and the results are also given in Table 1. It seems that the IFOS incorporation onto the silica materials is well performed through the template-free route.

The IFOS incorporation also depends upon role of emulsification and de-emulsification of reactant species. The percentage of hydrophobic and oleophobic nature can define the character of organosilane-reaction in polar medium, which play a key role in phase separation during self-assembly. This is exemplified by BImI_SiO$_2$, showing the influence of the counter anion. The bulky iodine counter ion ($Im^+ \rightarrow I^-$) stays far away from the aromatic imidazole ring, thus increasing the oleophobic nature of the medium. It can thus act as de-emulsification agent and decrease the influence of the by-product ethanol, and hence the resultant BImI_SiO$_2$ material shows a more bulky portion with less porosity. PImBr_SiO$_2$ offers further support in which the propyl group of the PImBr_SiO$_2$ shows oleophobicity lower than the butyl group of the BImBr_SiO$_2$, with facile incorporation of higher levels of IFOS as well as narrow size distribution.

The morphology of *n*-BImBr_SiO$_2$ characterized by SEM (Fig. 3) clearly shows the presence of spherical particles with a regular shape.

3.2. Cycloaddition of carbon dioxide to AGE by ionic liquid functionalized mesoporous silica (IFMS)

The synthesis of cyclic carbonate from the epoxide and CO_2 using the heterogeneous IFMS catalysts was carried out in a high-pressure batch reactor. Based on the reaction mechanism [40], the formation of the cyclic carbonate was initiated through the coordination of the IFMS with the epoxide. The rate-determining step was the attack at the anionic site of the catalyst, forming the five-membered bulky quaternary onium salt with the oxirane. The CO_2 then approaches the charged system and inserts into the ring, followed by construction of a new, four-membered cyclic ring that distributes the charge density and allows for creation of the final cyclic carbonate [41–45].

Table 2 shows conversion of AGE and selectivity to AGC and turnover number (TON) of AGC for three different immobilized IL catalysts at CO_2 pressure of 0.86–3.55 MPa. When the alkyl chain length increased from propyl (*n*-PImBr_SiO$_2$) to butyl (*n*-BImBr_SiO$_2$), the yield and TON of AGC increased mainly due to the more donating nature of the butyl group, having the capacity to pump electron density to the center of the active site, than that of the propyl group. When comparing the activity of the counter anion, iodide (*n*-BImI_SiO$_2$) showed a little higher AGC yield than bromide (*n*-BImBr_SiO$_2$) since *n*-BImI_SiO$_2$ has more nucleophilic I^- counter ion than Br^-. Considering the higher steric hindrance of I^- than Br^-, the effects of counter anion on the reactivity are combined phenomena of the nucleophilicity and steric hindrance. However, the TON of AGC was much higher for *n*-BImBr_SiO$_2$ since it had smaller amount of attached ionic liquid than *n*-BImI_SiO$_2$.

Table 2 also shows the effect of CO_2 pressure on the reactivity of the three immobilized catalysts. The AGE conversion and the yield of the cyclic carbonate increased as CO_2 pressure increased from 0.86 to 3.55 MPa. High CO_2 pressure could enhance the absorption of CO_2 in the solution of AGE. Zhang et al. [46] reported the increase

Table 1
The physico-chemical properties of IFMS.

Catalyst	ILs content[a] (mmol/g)	S_{BET} (m^2/g)	D_P[b] (Å)	V_P[b] (cm^3/g)	$S\mu_{BET}$[c] (m^2/g)	$V\mu_P$[c] (cm^3/g)
n-BImBr_SiO$_2$	0.61	477.4	42.0	0.4	40.0	0.01
n-BImI_SiO$_2$	0.93	188.9	31.6	0.1	19.3	0.01
n-PImBr_SiO$_2$	0.83	647.4	32.9	0.3	139.6	0.06

Synthesis condition: 0.818 TEOS:0.182 IFOS:5.61 HCl:153.9 H_2O, where TEOS/IFOS ratio was 4.5.

[a] Amount of immobilized ionic liquid calculated by the nitrogen content of elemental analysis.

[b] Pore diameter and pore volume measured by N_2 adsorption using *BJH* method.

[c] Micropore surface area and micropore volume were measured by *t*-plot method.

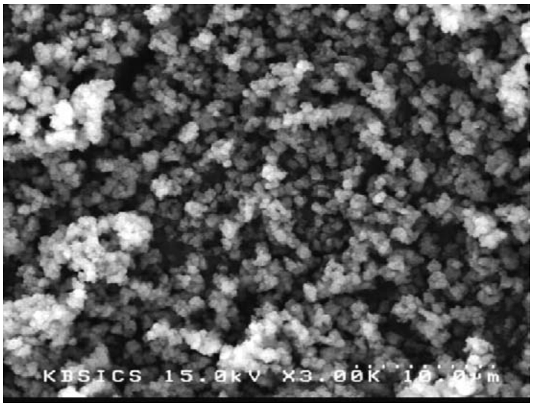

Fig. 3. SEM morphology of *n*-BImBr_SiO$_2$.

of the solubility of CO$_2$ in BMImPF$_6$ with increasing the pressure of CO$_2$. It is also reported, in the CO$_2$/cyclohexne oxide coupling reaction catalyzed by chromium salen complexes, that high CO$_2$ pressure increased turnover number of the reaction [47].

The advantages of present study are supported by previous reports. The conventional ion-exchange resin (Dowex MSA-1) did not yield impressive results next to poly(4-vinylpyridine)-ZnBr$_2$, which exhibits only 53% yield, even when polymers were coupled after ZnBr$_2$. Moreover, similar cross linked poly(4-vinylpyridine)-ZnBr$_2$ showed 33% yield [13]. While considering the Mg–Al mixed oxide catalyst, high yields of cyclic carbonates were obtained at 100 °C, even at low carbon dioxide pressure [20], however, this catalyst system needs a highly polar amide solvent such as *N*,*N*-dimethylformamide that is difficult to separate at milder conditions, making the system homogenous and non-cost-effective when compared to that of the current, more economical, solvent-free system. A silica-supported chromium-salen complex catalyst can catalyze this reaction [48], but higher reaction temperatures and CO$_2$ pressures were required when compared to this catalyst system. Thus, the present catalyst system is not only effective but has great potential in industry from the standpoint of cost.

Table 3 shows the effect of reaction temperature and reaction time on the conversion of AGE and selectivity to AGC using *n*-BImBr_SiO$_2$ catalyst. The conversion of AGE and selectivity to the cyclic carbonate increased as the temperature increased from 60 °C to 120 °C. It means that there is no severe decomposition of the cyclic carbonate to AGE and CO$_2$ even at 120 °C during 6 h of reaction. However it decreased at 140 °C, probably due to the partial decomposition of the cyclic carbonate to monomer AGE at high temperature. Table 3 also shows that at 110 °C, the AGE conversion increased continuously from 0.5 to 6 h of reaction.

Table 2
The reactivity of different IFMS catalysts for the cycloaddition of carbon dioxide to AGE.

Catalyst	Pressure (MPa)	Conversion of AGE (%)	Selectivity to AGC (%)	TON for AGC[a]	TOF for AGC[b]
n-BImBr_SiO$_2$	0.86	55.1	93.4	66.6	11.1
	1.76	85.3	87.3	97.0	16.2
	3.55	99.1	92.5	119.4	19.9
n-BImI_SiO$_2$	0.86	58.4	87.9	44.4	7.4
	1.76	95.4	94.6	78.0	13.0
	3.55	98.7	94.8	80.8	13.5
n-PImBr_SiO$_2$	0.86	50.8	43.1	21.1	3.5
	1.76	88.5	91.9	78.3	13.0
	3.55	98.5	91.8	87.0	14.5

Reaction condition: amount of AGE = 40 mmol, reaction time = 6 h, temperature = 110 °C, CO$_2$ pressure = 0.86–3.55 MPa.

[a] Turnover number as mole of AGC/mole of IL in catalyst.

[b] TOF = TON/reaction time (h^{-1}).

Table 3
The effect of reaction time and temperature on the conversion of AGE and selectivity to AGC for *n*-BImBr_SiO$_2$.

Temperature (°C)	Pressure (MPa)	Time (h)	Conversion of AGE (%)	Selectivity to AGC (%)
80	0.86	6	33.0	85.6
100	0.86	6	44.2	88.9
120	0.86	6	63.3	93.4
140	0.86	6	51.9	79.2
110	1.76	0.5	9.1	49.2
110	1.76	1	27.9	70.4
110	1.76	3	77.1	80.7
110	1.76	6	85.3	87.3

Reaction condition: catalyst = 0.5 g, AGE = 40 mmol, reaction time = 0.5–6 h, temperature = 80–140 °C, CO$_2$ pressure = 0.86–1.76 MPa.

Table 4
The effect of ZnBr$_2$ co-catalyst on the conversion of AGE and selectivity of AGC for *n*-BImBr_SiO$_2$.

Catalyst (mmol)	Co-catalyst (mmol)	Conversion of AGE (%)	Selectivity to AGC (%)
n-BImBr_SiO$_2$ (2)	–	60.2	86.7
n-BImBr_SiO$_2$ (2)	ZnBr$_2$ (0.5)	68.5	90.5
n-BImBr_SiO$_2$ (2)	ZnBr$_2$ (1)	84.9	92.3
BImBr (2)	–	41.0	68.5

Reaction condition: AGE = 40 mmol, reaction time = 6 h, temperature = 110 °C, CO$_2$ pressure = 0.86 MPa.

Table 4 shows the effect of zinc bromide co-catalyst on the cycloaddition of CO$_2$ to AGE. ZnBr$_2$ alone showed no activity for this reaction. The mixture of zinc bromide with *n*-BImBr_SiO$_2$ showed an enhanced effect in AGE conversion compared to the *n*-BImBr_SiO$_2$ itself. The increased activity of *n*-BImBr_SiO$_2$ with ZnBr$_2$ may originate from the cooperative action of both the acidic site (Zn) for epoxide activation and basic site (Br$^-$ in *n*-BImBr_SiO$_2$ and/or Br$^-$ in ZnBr$_2$) for CO$_2$ activation, as reported previously by Sun et al. [49] for the synthesis of styrene carbonate from styrene oxide and carbon dioxide. Fuwei et al. [50] also reported an increase of the yield of propylene carbonate from propylene oxide and CO$_2$ with the use of ZnBr$_2$ co-catalyst.

The influence of the amount of BImBr in the mixed catalyst was also studied with the ratios of *n*-BImBr_SiO$_2$/ZnBr$_2$ from 2 to 4. The mixed catalyst with *n*-BImBr_SiO$_2$/ZnBr$_2$ = 2 showed higher AGE conversion than BImBr_SiO$_2$/ZnBr$_2$ = 4. It confirms that two moles of ionic liquid and one mole of ZnBr$_2$ will form the metal-IL complex as suggested by the mechanism proposed by Zhang et al. [32].

A series of catalytic cycles were carried out to investigate the stability of the immobilized ionic liquid catalyst. In each cycle, the catalyst was separated by filtration and then used directly for the next run. Table 5 shows the activity of the reused *n*-BImBr_SiO$_2$ catalyst. It shows that the catalyst can be reused at least up to three consecutive times with only a slight loss of its activity and selectivity.

Table 5
Reactivity of recycled *n*-BImBr_SiO$_2$ catalyst.

Recycle no	Conversion of AGE (%)	Selectivity to AGC (%)
Fresh	99.1	92.5
1	97.7	91.1
2	95.3	90.4
3	94.4	88.4

Reaction conditions: AGE = 40 mmol, Catalyst = 0.5 g, reaction time = 6 h, temperature = 110 °C, CO$_2$ pressure = 3.55 MPa.

4. Conclusion

Functionalized silica materials were prepared by a simple co-condensation of TEOS with IFOS under acidic conditions. The resultant materials with the solvent extraction-free system contained mesoporous structures with narrow pore size distributions. In the synthesis of cyclic carbonate from AGE and carbon dioxide, the immobilized ionic liquid (Im-IL) on amorphous silica showed good catalytic activity without using any solvent. The ionic liquid of larger alkyl chain structure and more nucleophilic anion exhibited better reactivity for the cycloaddition of carbon dioxide and AGE. High temperature, long reaction time, and high CO_2 pressure also increased the conversion of AGE. The use of zinc bromide co-catalyst with the ionic liquid enhanced the reactivity due to the cooperative action of both the acidic site (Zn) and basic site (Br^-). The Im-IL on amorphous silica can be easily recovered and reused without any considerable loss of its initial activity.

Acknowledgements

This study was supported by the Korea Science and Engineering Foundation (2009-0053022), KBSI and the Brain Korea 21 Project.

References

[1] D.J. Darensbourg, M.W. Holtcamp, Coord. Chem. Rev. 153 (1996) 155.
[2] X.D. Xu, J.A. Moulijin, Energy Fuels 10 (1996) 305, and references therein.
[3] D.H. Gibson, Coord. Chem. Rev. 185–186 (1999) 335.
[4] M. Shi, Y.-M. Shen, Curr. Org. Chem. 7 (2003) 737.
[5] S. Inoue, N. Yamazaki, Organic and Bioorganic Chemistry of Carbon Dioxide, Kodansha Ltd, Tokyo, 1981.
[6] G. Rokicki, W. Kuran, B.P. Marciniak, Monatsh. Chem. 115 (1984) 205.
[7] E.H. Lee, J.Y. Ahn, M.D. Manju, D.W. Park, S.W. Park, I. Kim, Catal. Today 131 (2008) 130.
[8] M.S. Super, E.J. Beckman, Trends Polym. Sci. 5 (7) (1997) 236.
[9] D.J. Darensbourg, R.M. Mackiewiicz, A.L. Phelps, D.R. Billodeaux, Acc. Chem. Res. 37 (2004) 836.
[10] G.W. Coates, D.R. Moore, Angew. Chem. Int. Ed. 43 (2004) 6618.
[11] H. Sugimoto, S. Inoue, J. Polym. Sci. A: Polym. Chem. 42 (2004) 5561.
[12] M. Aresta, A. Dibenedetto, Dalton Trans. (2007) 2975.
[13] H.S. Kim, J.J. Kim, H.N. Known, M.J. Chung, B.G. Lee, H.G. Jang, J. Catal. 205 (2002) 226.
[14] H. Yasuda, L.N. Hen, T. Sakakura, J. Catal. 209 (2002) 547.
[15] W.J. Kruper, D.V. Dellar, J. Org. Chem. 60 (1995) 725.
[16] N. Kihara, N. Hara, T. Endo, J. Org. Chem. 58 (1993) 6198.
[17] G. Rokicki, W. Kuran, Bull. Chem. Soc. Jpn. 57 (1984) 1662.
[18] R. Nomura, A. Ninagawa, H. Matsuda, J. Org. Chem. 45 (1980) 3735.
[19] T. Yano, H. Matsui, T. Koike, H. Ishiguro, H. Rujihara, M. Yoshihara, T. Maeshima, Chem. Commun. (1997) 1129.
[20] K. Yamaguchi, K. Ebitani, T. Yoshida, H. Yoshida, K. Kaneda, J. Am. Chem. Soc. 121 (1999) 4526.
[21] J.J. Peng, Y. Deng, New J. Chem. 25 (2001) 639.
[22] T. Aida, S. Inoue, J. Am. Chem. Soc. 105 (1983) 1304.
[23] R.L. Addock, S.T. Nguyen, J. Am. Chem. Soc. 123 (2001) 11498.
[24] K. Kasuga, S. Nagao, T. Fukumoto, M. Handa, Polyhedron 15 (1996) 69.
[25] H. Yasuda, L. He, T. Sakakura, C. Hu, J. Catal. 233 (2005) 119.
[26] H. Kawannmi, Y. Ikushima, Chem. Commun. (2003) 896.
[27] L.-F. Xiao, F.-W. Li, J.-J. Peng, C.-G. Xia, J. Mol. Catal. A: Chem. 253 (2006) 265.
[28] R. Srivastava, D. Srinivas, P. Ratnasamy, Micropor. Mesopor. Mater. 90 (2006) 314.
[29] R. Srivastava, D. Srinivas, P. Ratnasamy, Tetrahedron Lett. 47 (2006) 4213.
[30] T. Welton, Chem. Rev. 99 (1999) 2071.
[31] C.E. Song, W.H. Shim, E.J. Roh, J.H. Choi, Chem. Commun. (2000) 1695.
[32] S. Zhang, Y. Chen, F. Li, X. Lu, W. Dai, R. Mori, Catal. Today 115 (2006) 61.
[33] K.R. Seddon, Kinet. Catal. 37 (1996) 693.
[34] A.S. Larsen, J.D. Holbery, F.S. Tham, C.A.J. Reed, J. Am. Chem. Soc. 122 (2000) 7264.
[35] S. Udayakumar, H.L. Shim, M.K. Lee, S.W. Park, D.W. Park, Catal. Commun. 10 (2009) 659.
[36] E. Cano-Serrano, G. Blanco-Brieva, J.M. Campos-Martin, J.L.G. Fierro, Langmuir 19 (2003) 7621.
[37] R.D. Badley, W.T. Ford, J. Org. Chem. 54 (1989) 5437.
[38] J.E.G. Mdoe, J.H. Clark, D.J. Macquarrie, Synlett (1998) 625.
[39] K. Shimizu, E. Hayashi, T. Hatamachi, T. Kodama, Y. Kitayama, Tetrahedron Lett. 45 (2004) 5135.
[40] H.L. Shim, MS Dissertation, Pusan National University, Busan, Korea, 2009.
[41] N. Kihara, N. Hara, T. Endo, J. Org. Chem. 58 (1993) 6198–6202.
[42] T. Aida, S. Inoue, J. Am. Chem. Soc. 105 (1983) 1304–1309.
[43] G. Rokocki, J. Pawlicki, W. Kuran, J. Polymer 17 (1985) 509–516.
[44] N. Kihara, T. Endo, Macromolecules 25 (1992) 4824–4825.
[45] T. Nishikubo, A. Kameyama, J. Yamashima, T. Fukumitsu, C. Maejima, M. Tomoi, J. Polym. Sci., Part A: Poly. Chem. 33 (1995) 1011–1017.
[46] S. Zhang, X. Yuan, Y. Chen, X. Zhang, J. Chem. Eng. Data 50 (2005) 1582.
[47] D.J. Darensbourg, R.M. Mackiewicz, D.R. Billodeux, Organometallics 24 (2005) 144.
[48] M. Ramin, F. Jutz, J. Grunwaldt, A. Baiker, J. Mol. Catal. A: Chem. 242 (2005) 32.
[49] J. Sun, S.-I. Fujita, F. Zhao, M. Arai, Green Chem. 6 (2004) 613.
[50] L. Fuwei, X. Linfei, X. Chungu, H. Bin, Tetrahedron Lett. 45 (2004) 8307.